Addressable photocharging of single quantum dots assisted with atomic force microscopy probe

M. Dokukin, R. Olac-Vaw, N. Guz, V. Mitin, and I. Sokolov

Addressable photocharging of single quantum dots assisted with atomic force microscopy probe

M. Dokukin,[1] R. Olac-Vaw,[2] N. Guz,[1] V. Mitin,[2] and I. Sokolov[1,a]

[1]*Department of Physics, Clarkson University, Potsdam, New York 13699-5820, USA*
[2]*Department of Electrical Engineering, University of Buffalo, The State University of New York, Buffalo, New York 14260-1920, USA*

Here we report on addressable photocharging of individual cadmium selenide quantum dots (QDs). The charging is a result of synergetic action of light and an atomic force microscope (AFM) probe. The probe squeezes the coating layer of QDs helping the photoelectron to tunnel to either conductive AFM probe or substrate. The charge can be induced on individual QDs by locating the QDs with AFM. The charges are stable in ambient conditions. These results may be of interest for QDs based sensors, memory, and solar cell applications. For instance, this method could provide recording information at a density of 1 Tb/cm^2. © 2009 American Institute of Physics. [doi:10.1063/1.3254895]

Nontrivial photonic and electrical properties of quantum dots (QDs) (Refs. 1 and 2) have attracted great attention to this material as a promising candidate for quantum information processing,[3] thin-film devices, nanoscale lasers,[4–6] flexible polymeric solar cells,[7] etc. Cadmium selenide (CdSe) nanocrystals are one of the most popular QDs.[8–10]

Atomic force microscope (AFM) is a powerful tool to study, image, and manipulate nanoscopic systems.[11,12] Several AFM techniques allow measuring electrostatic force between a sample and conductive AFM tip. Such techniques were used to measure the motion of single electron charges,[13] charges on bacterium surfaces,[14] imaging of the flow of electron waves around a single-electron quantum dot,[15] charges on quantum dots.[16] Here we use the AFM technique with a dual purpose, to assist photocharging of individual QDs and to measure the value of the induced electrical charge on each QD. Because the AFM probe can easily be positioned with a sub nanometer precision, this method can be applied for addressable charging of individual QDs.

Here we found that the presence of an AFM probe accelerates the induction of a positive charge in QDs, which are capped with tri-n-octylphosphineoxide (TOPO) layer, and deposited on a highly ordered pyrolytic graphite film (graphene). A schematic of the experiment is shown in Fig. 1. A conductive AFM probe scans over QDs deposited on graphite surface, Fig. 1(a). The scanning is done in the ac lift mode.[17] The presence of an electrical charge q results in the following shift Δf of the resonance frequency f of the cantilever:

$$\Delta f = \frac{q^2 f}{8\pi k \varepsilon_0} \cdot \frac{a(a^2 + 3z^2)}{(z^2 - a^2)^3} + \frac{f}{2k}\frac{\partial F_C}{\partial z}, \qquad (1)$$

where $F_C = 1/2(V_{DC} - \phi)^2 \partial C/\partial z$. Here C is the capacitance of QD, V_{DC} is the bias dc voltage applied to the conducting AFM probe, ϕ is the potential difference between the probe and substrate, ε_0 is the dielectric permeability of vacuum, k is the spring constant of the AFM cantilever, a is the AFM probe radius, and $z = h + a - x$, h is the distance between the

probe and a point charge (positioned at the center of QD), Fig. 1(b), x is a possible elastic deformation of the substrate. Contribution of the mirror charges induced in the substrate are negligible.

The biased voltage between the probe and graphene film was set to eliminate additional capacitive force described by the second term of Eq. (1). A transmission electron microscopy image of the used quantum dots is shown in the top of Fig. 1(c). One can see a few nanometer TOPO coating. Figure 1(c) middle shows an AFM image of QDs dispersed on graphite surface. One can see both individual QDs and larger
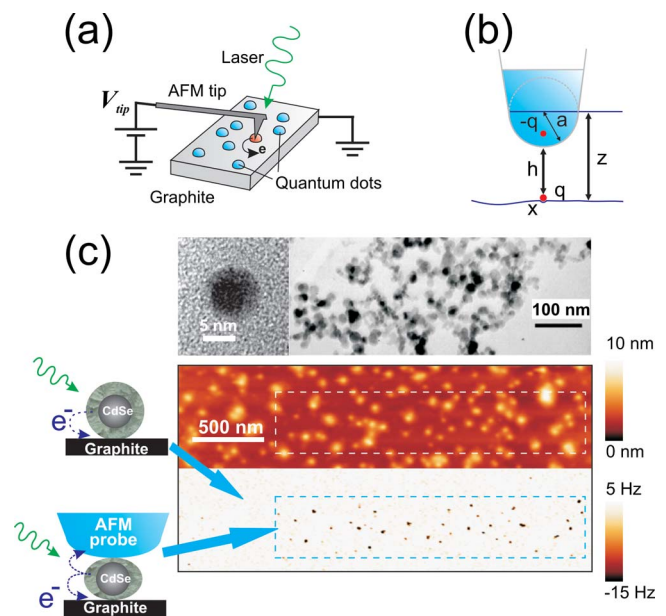
FIG. 1. (Color online) AFM probe-assisted photocharging of QDs. (a) Experimental setup. QDs dispersed onto graphene film. Electrons in QDs are photoexcited with a green laser. (b) A schematic of the AFM probe-QD interaction. CdSe nanocrystal is shown as a point charge **q**. (c) Top: TEM images of dispersed TOPO capped CdSe nanocrystal QDs; middle: a topographic AFM image of the dispersed QDs; bottom: the change of resonance frequency over the same area as shown on the top image. The region inside a dashed rectangle is the area in which the AFM probe scanned the surface during illumination with the laser. Schematics of QDs illuminated by laser without and with touching with the AFM probe are shown on the left.

a)Electronic mail: isokolov@clarkson.edu.

clusters. The bottom image shows the AFM map of Δf, i.e., charges. This AFM scan was collected as follows. The entire area was continuously illuminated with laser for ~ 10–15 minutes. Simultaneously, the AFM scans within a small region outlined by a dashed rectangle shown in Fig. 1(c). After this scan, the laser was switched off, and a larger area was scanned. The dark sports seeing inside the smaller area correspond to the decrease of the resonance frequency Δf, i.e., charges, see Eq. (1). Comparing the position of QDs and the location of the dark spots, one can see that the charges are associated with the QDs. One can see that almost all these charges are located within the rectangle small area of the initial AFM scanning. Thus, we can conclude that the AFM probe assisted in charging the QDs. It should be noted, however, that QDs can gain photoinduced charges and without the action of the AFM if the laser illumination is sufficiently long. For example, in our experiments it took ~ 40–50 minutes of continuous illumination of QDs to obtain charge images similar to the shown in Fig. 1(c). Thus, we attribute the acceleration of the photoionization of QDs to the presence of AFM probe.

To understand the nature of this phenomenon, we hypothesize that it may happen because of the two following possible reasons: (1) The AFM probe works as a sort of antenna collecting light and creating enhanced electromagnetic field at its apex, a phenomenon similar to the tip enhanced Raman spectroscopy; (TERS)[18] and (2) Due to the enhanced tunneling. To work as a TERS antenna, the AFM probe had to be noticeably smaller than the probe used here. The second mechanism is schematically shown in Fig. 1(c), on the left. When a QD is just sitting on graphene, photoexcitation creates a free electron, which could tunnel through the TOPO layer. When the AFM probe touching the QD, it squeezes the TOPO layer, the width of the potential barrier decreases, and consequently, the electron has higher probability to tunnel to either the probe or graphite. In principle, the area of contact between the conductive surfaces (the probe and substrate) and QDs may slightly increase during the taping mode used here for imaging. However, it results in a just minor change in the tunneling probability compared to the change due to the decrease of the barrier thickness (linear versus exponential contributions, respectively). Below we show that the observed accelerating charging can presumably be explained with the help of this mechanism.

We first find the amount of charge induced in each QD. Figure 2(a) shows an example of Δf (charge) images obtained over sufficiently large area. Collecting a statistical amount of Δf for individual QDs when scanning in different lift heights (probe-QD distances), one gets the results shown in Fig. 2(b). Fitting these data (for $h > 3.75$ nm) with Eq. (1) for two unknowns, x and q, one obtains the charge of QD $q = (1.0 \pm 0.2)e$, where e is the electron charge [$x = (0.47 \pm 0.59)$ nm]. Two dash lines shown in Fig. 2(b) correspond to Eq. (1) with the fitted data (1e) and when the charge was put to 2e. (It should be noted that the error due to inaccuracy in defining values a and h in Eq. (1) is within percents, which is smaller than variability of the experimental data.) One can clearly see that we are dealing with a single charge of electron. Intriguingly, there are no 2e charges observed. Some deviation from the theoretical curve is seen for smaller probe-QD distances. This is expected because the probe starts interacting sterically with the TOPO
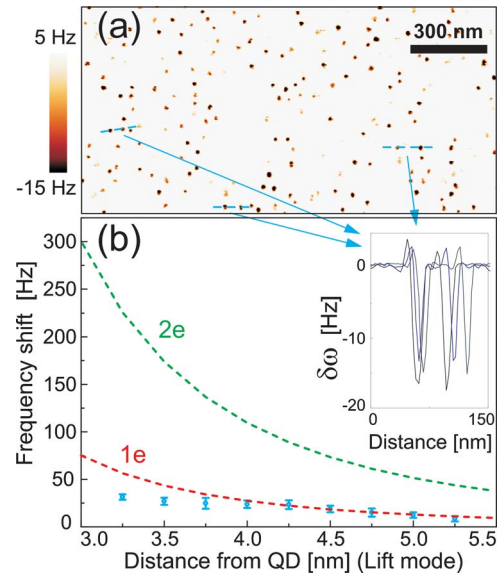

FIG. 2. (Color online) Estimation of the charge of QDs. (a) A map of Δf on a sample charged by synergetic 15-min action of the AFM probe and green laser. (b) Δf as a function of distance between the AFM probe and sample. Δf was averaged over single QDs of both image (a) and several other images (only well defined QDs where taken in consideration, if the size and height corresponded to a single QD). Variability bars correspond to one standard deviation. Two dashed lines show the theoretical predictions (Eq. (1)) for single and double electron charges. Inset demonstrates several cross-sections of Δf along the marked lines shown in (a).

layer, and subsequently, decreasing the charge attraction.

As demonstrated by compensating the charges with a flow of negative ions the induced charges are positive. It was also found that the charges are extremely robust. They can even recover within less than a minute after their forced neutralization by negative air ions. Typically, the charges disappear after 24 h.

We can now test our tunneling hypothesis to explain the observed accelerated charging. The AFM probe squeezes the TOPO layer, and consequently, increases tunneling probability of the electron from the QD through the TOPO layer to the nearest electron drain. The lifetime τ of an excited electron inside a QD can be estimated as[19]

$$\tau = \frac{R_{QD}}{v} \exp\left\{ \frac{2}{\hbar} \int_0^d \sqrt{2m[V(x) - E]}\, dx \right\}, \quad (2)$$

where R_{QD} is the radius of a QD (2.4 nm), v is an effective electron velocity, $E(m)$ is the electron energy (mass), and d is the thickness of the potential barrier. The potential barrier of the TOPO layer can be approximated by a linear potential $V(x) = (\Phi_1 - \Phi_2)x/d + \Phi_2 + V_0$, where Φ_1 (Φ_2) is the work function of the material that the tunneling electron leaves (tunnels to), and V_0 is an effective potential of the TOPO layer. V_0 gets an additional Coulomb energy term if the QD is charged.

The observed behavior can be summarized as follows: (1) The AFM-assisted charging of QDs happens within 10–15 minutes. During this time, the AFM probe scans over the area of ~ 1500 nm^2. While oscillating, it touches each individual QD for $\tau_1 \sim 0.2$ sec. (2) Without the probe assistance, it takes $\tau_2 = 40$–50 minutes for the photoexcited electrons to escape the QD. (3) Without photoexcitation, it takes $\tau_3 = 24$ hours for an electron to tunnel from the graphite substrate through the TOPO into the charged QD. Using these

three lifetime values, one can build two ratios. Because we do not change the material, and presumably do not deform each QD (core), pre-exponential factor in Eq. (2) will be canceled, and the ratios of τ_2/τ_1 and τ_3/τ_1 will depend only on the following unknown parameters: V_0 and Δd (the change of the thickness of TOPO layer). The integrals of Eq. (2) can be taken numerically using $E=h\nu-E_{QD}$, where $h\nu$ is the energy of exciting photon, $E_{QD}=1.96$ eV is the QD bandgap (estimated from fluorescence measurements), $d\sim2.1$ nm (from the TEM data, assuming three TOPO monolayers), and $\Phi_{CdSe}=5.35$ V, $\Phi_{Cr}=4.50$ V, $\Phi_{graphite}=4.65$ V). One can see that these two equations have a solution for the following values of $V_0\sim1.8$ eV and $\Delta d\sim0.11$ nm ($\sim5\%$ of the original thickness). Both parameters seem to be quite reasonable.

Before concluding, it is worth of discussing the reason of seeing just one charge of electron on QDs. The second photoexcited electron would require ~0.14 eV higher energy to leave the positively charged QD. With the parameters derived above from Eq. (2), this additional energy is negligible. Thus, the absence of two electronic charges should be related to the change in the bandgap structure of QDs. This is in agreement with a number of works, e.g.,[20] in which the appearance of dark and bright periods in the photoluminescent intensity of single CdSe nanocrystals was addressed to Auger photoionization of the QD followed by its neutralization. Such blinking occurs frequently in the organically capped dots, while inorganic capping reduces the ionization frequency and leads to longer on-period.[21]

In conclusion, we described a method of addressable photocharging of individual CdSe QDs deposited on a conductive substrate (graphite) in ambient conditions. An AFM probe squeezed the TOPO coating of QDs during scanning, which substantially accelerated the tunneling of the photoexcited electron from the QD to either conductive substrate or AFM probe. As a result each QD obtains the charge of +1e, which is rather robust and can survive ~24 hours in ambient conditions. Substantially higher lifetimes can be attained, for example, by taking thicker TOPO coatings as predicted by Eq. (2). As such, the effect can potentially be used for creation of QD-based sensors, high-density memory applications. For example, if we arrange QDs placed 10 nm from each other (the minimum distance in which QDs do not electromagnetically cross-talk), then 1 cm^2 would carry 1 Tb of

information. In the solar cell applications, the observed effect can rather be undesirable because the electrically charged QDs seem to be photoinactive (which is in agreement with the results of Ref. 20). So, the control of the absence of accumulated charges can be used for optimization of solar cell technology.

[1] D. J. Norris, A. Sacra, C. B. Murray, and M. G. Bawendi, Phys. Rev. Lett. **72**, 2612 (1994).

[2] D. V. Talapin, A. L. Rogach, A. Kornowski, M. Haase, and H. Weller, Nano Lett. **1**, 207 (2001).

[3] X. Xu, W. Yao, B. Sun, D. G. Steel, A. S. Bracker, D. Gammon, and L. J. Sham Nature, (London) **459**, 1105 (2009).

[4] V. I. Klimov, A. A. Mikhailovsky, D. W. McBranch, C. A. Leatherdale, and M. G. Bawendi, Science **287**, 1011 (2000).

[5] A. A. Mikhailovsky, A. V. Malko, J. A. Hollingsworth, M. G. Bawendi, and V. I. Klimov, Appl. Phys. Lett. **80**, 2380 (2002).

[6] V. I. Klimov, A. A. Mikhailovsky, S. Xu, A. Malko, J. A. Hollingsworth, C. A. Leatherdale, H.-J. Eisler, and M. G. Bawendi, Science **290**, 314 (2000).

[7] B. J. Landi, S. L. Castro, H. J. Ruf, C. M. Evans, S. G. Bailey, and R. P. Raffaelle, Sol. Energy Mater. Sol. Cells **87**, 733 (2005).

[8] G. Schlegel, J. Bohnenberger, I. Potapova, and A. Mews, Phys. Rev. Lett. **88**, 137401 (2002).

[9] S. A. Empedocles, D. J. Norris, and M. G. Bawendi, Phys. Rev. Lett. **77**, 3873 (1996).

[10] M. Nirmal, B. O. Dabbousi, M. G. Bawendi, J. J. Macklin, J. K. Trautman, T. D. Harris, and L. E. Brus, Nature (London) **383**, 802 (1996).

[11] A. J. M. Giesbers, U. Zeitler, S. Neubeck, F. Freitag, K. S. Novoselov, and J. C. Maan, Solid State Commun. **147**, 366 (2008).

[12] H. J. Butt, B. Cappella, and M. Kappl, Surf. Sci. Rep. **59**, 1 (2005); M. Firtel, G. Henderson, and I. Sokolov, Ultramicroscopy **101**, 105 (2004).

[13] M. T. Woodside and P. L. McEuen, Science **296**, 1098 (2002).

[14] I. Sokolov, D. S. Smith, G. S. Henderson, Y. A. Gorby, and F. G. Ferris, Environ. Sci. Technol. **35**, 341 (2001).

[15] P. Fallahi, A. C. Bleszynski, R. M. Westervelt, J. Huang, J. D. Walls, E. J. Heller, M. Hanson, and A. C. Gossard, Nano Lett. **5**, 223 (2005).

[16] T. D. Krauss and L. E. Brus, Phys. Rev. Lett. **83**, 4840 (1999).

[17] See EPAPS supplementary material at http://dx.doi.org/10.1063/1.3254895 for materials and methods.

[18] C. Georgi, M. Hecker, and E. Zschech, Appl. Phys. Lett. **90**, 171102 (2007).

[19] D. J. Griffiths, *Introduction to Quantum Mechanics*, 2nd ed. (Pearson Prentice Hall, Upper Saddle River, NJ, 2005), pp. ix, 468.

[20] R. G. Neuhauser, K. T. Shimizu, W. K. Woo, S. A. Empedocles, and M. G. Bawendi, Phys. Rev. Lett. **85**, 3301 (2000).

[21] Y. Yamasaki, H. Asami, T. Isoshima, I. Kamiya, and M. Hara, Sci. Technol. Adv. Mater. **4**, 519 (2003).